The $CysLT_2R$ receptor mediates leukotriene C_4-driven acute and chronic itch

Tiphaine Voisin[a], Caroline Perner[b], Marie-Angele Messou[a], Stephanie Shiers[c], Saltanat Ualiyeva[d,e], Yoshihide Kanaoka[d,e], Theodore J. Price[c], Caroline L. Sokol[b], Lora G. Bankova[d,e], K. Frank Austen[d,e,1], and Isaac M. Chiu[a,1]

[a]Department of Immunology, Blavatnik Institute, Harvard Medical School, Boston, MA 02115; [b]Center for Immunology & Inflammatory Diseases, Division of Rheumatology, Allergy and Immunology, Massachusetts General Hospital, Harvard Medical School, Boston, MA 02114; [c]Center for Advanced Pain Studies, School of Behavioral and Brain Sciences, University of Texas at Dallas, Dallas, TX 75080; [d]Division of Allergy and Clinical Immunology, Jeff and Penny Vinik Center for Allergic Disease Research, Brigham & Women's Hospital, Boston, MA 02115; and [e]Department of Medicine, Harvard Medical School, Boston, MA 02115

Contributed by K. Frank Austen, February 2, 2021 (sent for review October 26, 2020; reviewed by Diana M. Bautista and Bradley J. Undem)

Acute and chronic itch are burdensome manifestations of skin pathologies including allergic skin diseases and atopic dermatitis, but the underlying molecular mechanisms are not well understood. Cysteinyl leukotrienes (CysLTs), comprising LTC_4, LTD_4, and LTE_4, are produced by immune cells during type 2 inflammation. Here, we uncover a role for LTC_4 and its signaling through the CysLT receptor 2 ($CysLT_2R$) in itch. *Cysltr2* transcript is highly expressed in dorsal root ganglia (DRG) neurons linked to itch in mice. We also detected *CYSLTR2* in a broad population of human DRG neurons. Injection of leukotriene C_4 (LTC_4) or its nonhydrolyzable form $NMLTC_4$, but neither LTD_4 nor LTE_4, induced dose-dependent itch but not pain behaviors in mice. LTC_4-mediated itch differed in bout duration and kinetics from pruritogens histamine, compound 48/80, and chloroquine. $NMLTC_4$-induced itch was abrogated in mice deficient for *Cysltr2* or when deficiency was restricted to radioresistant cells. Itch was unaffected in mice deficient for *Cysltr1*, *Trpv1*, or mast cells (W^{Sh} mice). $CysLT_2R$ played a role in itch in the MC903 mouse model of chronic itch and dermatitis, but not in models of dry skin or compound 48/80- or *Alternaria*-induced itch. In MC903-treated mice, CysLT levels increased in skin over time, and $Cysltr2^{-/-}$ mice showed decreased itch in the chronic phase of inflammation. Collectively, our study reveals that LTC_4 acts through $CysLT_2R$ as its physiological receptor to induce itch, and $CysLT_2R$ contributes to itch in a model of dermatitis. Therefore, targeting CysLT signaling may be a promising approach to treat inflammatory itch.

itch | neuroimmune | atopic dermatitis | skin | inflammation

Itch, or pruriception, is defined as an uncomfortable sensation that triggers the desire to scratch, and is mediated by peripheral sensory neurons termed pruriceptors (1, 2). Increasing evidence indicates that inflammatory mediators are released into the skin by immune cells and other cell types that directly activate or sensitize pruriceptors to produce itch. Chronic itch is a debilitating symptom of many skin pathologies, including atopic dermatitis (AD) and allergic contact dermatitis (ACD), and the roles of individual molecular pathways in chronic itch are not clearly defined. While certain classes of mediators such as histamine, proteases, and cytokines have been investigated more recently, less is known about the roles of lipid mediators in itch. There is a great need for better understanding of the molecular mechanisms leading to itch and to develop novel therapeutic modalities to treat itch.

Leukotrienes (LTs) are eicosanoid lipid mediators generated upon activation of both immune and structural cells. LTs are comprised of LTB_4 and the cysteinyl LTs (CysLTs; LTC_4, LTD_4, and LTE_4; Fig. 1*A*). They were named "leukotrienes" to highlight their originally defined source: leukocytes, including mast cells (MCs), eosinophils, basophils, and macrophages (3). More recently, platelet–neutrophil aggregates (4) and tuft cells (5), which are specialized epithelial cells, were identified as potent producers of CysLTs, highlighting the ubiquitous and versatile sources of CysLTs during inflammation. The biosynthesis of LTs begins when arachidonic acid is liberated from membrane phospholipids and is converted into LTA_4 by the enzyme 5-lipoxygenase (5-LO) in the presence of the 5-LO–associated protein (FLAP; Fig. 1*A*). LTA_4 hydrolase processes LTA_4 into LTB_4, which binds to the LTB_4 receptors. LTC_4 synthase (LTC_4S), at the outer nuclear membrane, conjugates LTA_4 with reduced glutathione to produce LTC_4, the first and only intracellular CysLT (6). LTC_4 is rapidly transported extracellularly (within minutes) and converted sequentially by membrane-bound γ-glutamyl transferases and dipeptidases to LTD_4 and LTE_4. CysLTs exert their effects through three G protein-coupled receptors (GPCRs)—$CysLT_1R$, $CysLT_2R$, and $CysLT_3R$—with different affinities. $CysLT_1R$ and $CysLT_2R$, the receptors for the short-lived LTC_4 and LTD_4, are widely expressed in hematopoietic and structural cells. The stable end metabolite LTE_4 binds to the epithelial $CysLT_3R$ and mediates mucin release in response to the airborne fungus *Alternaria* (7, 8). Pharmacologic studies using heterologous transfectants indicated that $CysLT_1R$ is the high-affinity receptor for LTD_4 and binds LTC_4 with lesser affinity. By contrast, $CysLT_2R$ binds LTC_4 and LTD_4 at equimolar concentrations (9, 10). However, in vivo selectivity for LTC_4 and LTD_4 differ depending on the tissue distribution, frequency of CysLT

Significance

Interactions between the nervous system and immune system are central regulators of chronic itch, a key feature of pathologies like atopic dermatitis and allergic contact dermatitis. Cysteinyl leukotrienes (LTC_4, LTD_4, and LTE_4) are eicosanoid lipids known for mediating inflammation, bronchoconstriction, and vascular leakage. We demonstrate here that CysLTs are potent itch inducers and that this effect depends on the specific coupling of LTC_4 with its receptor $CysLT_2R$, which is expressed in a population of peripheral sensory neurons in the mouse and in human. We show that the LTC_4/$CysLT_2R$ pathway contributes to a model of chronic itch, suggesting that $CysLT_2R$ could be a new therapeutic target for intractable chronic itch.

Author contributions: T.V., Y.K., L.G.B., K.F.A., and I.M.C. designed research; T.V., C.P., M.-A.M., S.S., S.U., T.J.P., C.L.S., and L.G.B. performed research; K.F.A. contributed new reagents/analytic tools; T.V., C.P., M.-A.M., S.S., S.U., T.J.P., C.L.S., L.G.B., and I.M.C. analyzed data; and T.V., L.G.B., K.F.A., and I.M.C. wrote the paper.

Reviewers: D.M.B., University of California, Berkeley; and B.J.U., Johns Hopkins Asthma and Allergy Center.

The authors declare no competing interest.

[1]To whom correspondence may be addressed. Email: fausten@research.bwh.harvard.edu or isaac_chiu@hms.harvard.edu.

This article contains supporting information online at https://www.pnas.org/lookup/suppl/doi:10.1073/pnas.2022087118/-/DCSupplemental.

Published March 22, 2021.

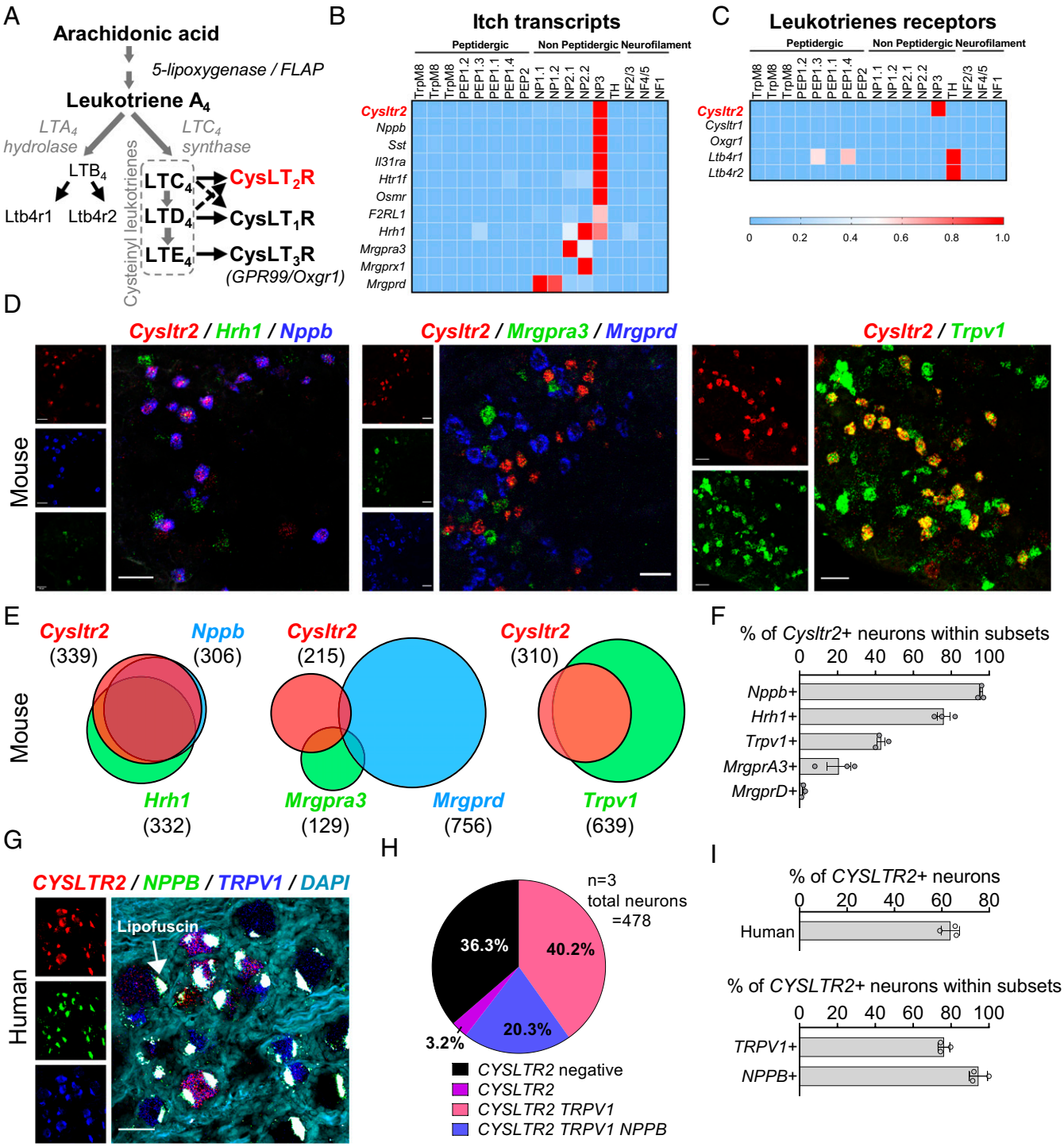

Fig. 1. *Cysltr2* is expressed on a subset of DRG sensory neurons. (*A*) Diagram of the LT pathway. (*B* and *C*) Expression of selected transcripts (*B*, related to itch; *C*, LT receptors) in mouse DRG neuron populations clustered into functional subsets based on single-cell RNA-seq data. Full dataset and methods are available in a previous study (32). (*D*) Triple/double-label ISH done with RNAscope in DRG (*Left*, *Cysltr2*, red; *Nppb*, blue; *Hrh1*, green; *Middle*, *Cysltr2*, red; *MrgprA3*, green; *Mrgprd*, blue; *Right*, *Cysltr2*, red; *Trpv1*, green). (Scale bar: 50 μm.) (*E* and *F*) ISH quantification: (*E*) Venn diagram representing overlap between markers and (*F*) percentages of *Cysltr2*$^+$ neurons within subsets defined by other markers ($n = 3$ mice). (*G*) Representative images of human DRG labeled with RNAscope ISH for *CYSLTR2* (red), *NPPB* (green), and *TRPV1* (blue) and costained with DAPI (cyan). Lipofuscin (globular structures) that autofluoresced in all three channels and appear white in the overlay image were not analyzed, as this is background signal that is present in all human nervous tissue. (Scale bar: 50 μm.) (*H*) Pie chart displaying the distribution of *CYSLTR2* neuronal subpopulations in human DRG. (*I*) Percentage of all human sensory neurons expressing *CYSLTR2* transcript (*Top*) and of *TRPV1* neurons and *NPPB* neurons coexpressing *CYSLTR2* (*Bottom*). Values presented as mean ± SEM.

receptor-expressing cells, and proximity to the ligand source (11–14). The brief half-life of LTC_4 within the tissue likely requires close proximity between the LTC_4 source and the target cell. CysLTs are potent inducers of airway smooth muscle constriction, vascular permeability, leukocyte recruitment, and chemokine production (3). Classically, the proinflammatory effects of CysLTs are attributed to the $CysLT_1R$ receptor, which participates in the recruitment of eosinophils, the activation of ILC2s, and Th2 response during airway inflammation (12, 15, 16). The $CysLT_1R$-specific antagonist montelukast is widely used to treat bronchoconstriction and inflammation in asthmatic patients (17, 18). $CysLT_2R$ is resistant to montelukast, and its role is not understood as well as $CysLT_1R$. $CysLT_2R$ signaling in platelets is required for type 2 lung inflammation and MC activation (19). Additionally, $CysLT_2R$ has a newly defined role in lung metastasis through an effect on angiogenesis (20). Eosinophil-derived LTC_4 also mediates skin fibrosis and inflammation through $CysLT_2R$ in an ovalbumin-induced mouse model of AD (14). Several groups have worked to elucidate the role of LTB_4 and its receptors in pain and itch (21–24). However, the role of CysLTs and their associated receptors in itch has not been well studied. Recent transcriptome studies suggest *Cysltr2* to be expressed in sensory neurons, but how $CysLT_2R$ regulates neural responses and itch behavior in vivo has not been clarified.

Pruriceptors are primary sensory neurons that mediate itch, whose cell bodies reside in the dorsal root ganglia (DRG) and trigeminal ganglia (25). Pruriceptors express molecular receptors at their peripheral nerve terminals in epidermal layers of the skin that respond to pruritogens including histamine, cytokines, and proteases. HRH1 and HRH4 are the major histamine receptors linked to pruriceptor activation and itch (26, 27). IL-4, IL-13, and IL-31 are cytokines that mediate itch via their cognate receptors expressed by pruriceptors (28, 29). Chloroquine (CQ) and BAM8-22, an endogenous peptide derived from proenkephalin, act via the Mas-related G protein receptors MrgprA3 and MrgprC11, respectively, to produce itch (30). Recent transcriptomic analyses have revealed distinct subsets of DRG neurons that may correspond to distinct pruriceptor subtypes and function, known as NP1, NP2, and NP3 neurons (31, 32). NP1 neurons express *Mrgprd* that responds to β-alanine to produce itch (33); NP2 neurons express *Mrgpra3* and *Mrgprc11* (30); NP3 neurons express *Il31ra* and *Osmr* (Oncostatin M receptor), which bind the pruritogenic cytokine IL-31 (28). NP3 neurons are also characterized by expression of neuropeptides *Nppb* and *Sst*, which have both been functionally linked to neurotransmission in itch (34–36).

In our molecular analysis as well in published datasets from other groups, we find that *Cysltr2* is highly enriched in the NP3 subset of DRG neurons (31, 32). However, the functional role of $CysLT_2R$ in pruriception, and the role of specific CysLTs (LTC_4, LTD_4, LTE_4) in itch, are unknown. Given that CysLTs are characteristic of type 2 immune cell activation in tissues during allergies, neuronal $CysLT_2R$ could allow the immediate response and induction of itch coupled to allergic-type inflammation.

In this study, our goal was to determine the functional role of specific CysLTs and $CysLT_2R$ in itch induction and skin inflammation. We find that *Cysltr2* is enriched in pruriceptor-lineage DRG sensory neurons in mouse and is also expressed in human DRG neurons. LTC_4, but not LTD_4 or LTE_4, induces acute itch behaviors in mice that differ in duration and quality from other pruritogens. We demonstrate that LTC_4-induced itch is dependent on the $CysLT_2R$ receptor. Bone-marrow chimeras show that radioresistant cells expressing $CysLT_2R$ are necessary for LTC_4-induced itch. Levels of LTC_4 are elevated in the late stage of a mouse model of chronic dermatitis and itch, and $Cysltr2^{-/-}$ mice have a decreased scratching phenotype at this time point. By contrast, $CysLT_2R$ did not mediate itch in other inflammatory skin models that we tested. Overall, our findings show that CysLTs play a role in itch in acute and chronic situations by acting through the $CysLT_2R$ receptor.

Results

Expression of *Cysltr2* Receptor in a Pruriceptive Subset of DRG Neurons. Molecular and genetic analysis of DRG neurons has recently identified distinct neurons linked to itch and other somatosensory functions (31, 37, 38). We previously performed single-cell profiling of FACS-sorted Nav1.8-lineage and Parvalbumin-lineage mouse DRG neurons (39). We observed a population cluster (VI) from Nav1.8-lineage neurons with enriched levels of itch-associated transcripts including *Il31ra*, the receptor for the cytokine IL-31 that drives pruritus (28, 40), and *Nppb*, a neuropeptide that mediates neurotransmission of itch signaling from DRG to the spinal cord (36). We found that *Cysltr2*, the receptor for LTC_4, was highly expressed in the same neuronal subset (*SI Appendix*, Fig. S1*A*). Other recently published single-cell RNA sequencing datasets of mouse DRG neurons revealed similar expression of *Cysltr2* in a population of neurons expressing *Il31ra*, *Nppb*, *Hrh1*, and *Sst*, termed NP3 neurons (31, 32, 38, 41). The $Cysltr2^+$ population is distinct from neurons expressing *Mrgpra3* or *Mrgprd* (Fig. 1*B*), markers of NP2 and NP1 neurons, respectively (42).

CysLTs are synthesized as part of arachidonic acid metabolism, where LTA_4 is processed by LTC_4S into LTC_4, which is subsequently metabolized to LTD_4 and LTE_4 (Fig. 1*A*). These ligands bind with different affinities to the receptors $CysLT_1R$, $CysLT_2R$, or $CysLT_3R$ (Oxgr1). Our analysis of the publicly available mouse RNA-sequencing (RNA-seq) dataset showed that *Cysltr2* was the only CysLT receptor expressed in sensory neurons, as transcripts for *Cysltr1* and *Oxgr1* were not detected (Fig. 1*C*). *Ltb4r1* and *Ltb4r2*, the receptors for LTB_4, were absent from pruriceptors but highly expressed in tyrosine hydroxylase (TH) neurons, a population of unmyelinated low-threshold mechanoreceptors (C-LTMRs) characterized by the expression of TH and associated with pleasant touch; *Ltb4r1* was additionally expressed in peptidergic subsets (PEP1.3 and PEP1.4; Fig. 1*C*). These data led us to focus on analysis of the role of $CysLT_2R$ in itch signaling.

To confirm the presence of *Cysltr2* transcript in mouse DRG neurons, we performed RNAscope in situ hybridization analysis. *Cysltr2* was expressed in 9.4 ± 1.9% of neurons marked by neuronal markers *Tubb3* (β-3 tubulin) and in 11.6 ± 2.2% of neurons marked by *Scn10a* (Nav1.8; *SI Appendix*, Fig. S1 *C* and *D*). *Cysltr2* overlapped extensively with *Nppb*: 95.7 ± 0.9% of $Nppb^+$ neurons were $Cysltr2^+$, whereas 86.0 ± 3.1% of $Cysltr2^+$ neurons are also $Nppb^+$ (Fig. 1 *D*–*F*). While still overlapping, 76.0 ± 3.2% of $Cysltr2^+$ neurons were $Hrh1^+$ and 74.7 ± 3.3% of $Hrh1^+$ neurons were $Cysltr2^+$, which confirms that the histamine receptor H1 is not completely restricted to the NP3 population (41). RNAscope analysis confirmed that *Mrgpra3*, which marks NP2 neurons, and *Mrgprd*, which marks NP1 neurons, had very little overlap with $Cysltr2^+$ neurons (Fig. 1 *D*–*F*), with 10.3 ± 3.2% and 7.0 ± 1.6% of $Cysltr2^+$ neurons being, respectively, $Mrgpra3^+$ and $Mrgprd^+$, and, inversely, 20.7 ± 6.4% of $Mrgpra3^+$ neurons and 2.0 ± 0.6% of $Mrgprd^+$ neurons being $Cysltr2^+$. The transient receptor potential (TRP) channel TrpV1 has been shown to play a role in histamine-dependent itch (26). RNA-seq data show that this ion channel is expressed in NP3 neurons (*SI Appendix*, Fig. S1*B*). Using RNAscope, we confirmed that the majority of $Cysltr2^+$ neurons (87.3 ± 2.2%) were $Trpv1^+$, while 43.0 ± 2.1% of $Trpv1^+$ neurons are $Cysltr2^+$ (Fig. 1 *D*–*F*).

A recent study performed developmental analysis of DRG neurons at the single-cell level to examine the evolution of transcript expression in sensory neurons at different stages of mouse development (*SI Appendix*, Fig. S1 *E* and *F*) (38). Our analysis of this database showed that DRG neurons started expressing *Cysltr2* after postnatal day 0 (*SI Appendix*, Fig. S1 *E* and *F*), and that it remained restricted to the same lineage of Sst^+ neurons from the moment it was expressed into adulthood (*SI Appendix*, Fig. S1*F*).

NEUROSCIENCE

We next characterized the expression of *CYSLTR2* in human DRGs using RNAscope analysis (Fig. 1*G* and *SI Appendix*, Fig. S1*G*). We found that 63.6 ± 2.2% of human DRG neurons expressed *CYSLTR2* (Fig. 1 *G*–*I*), which is broader in expression than in mouse, and these neurons ranged in size from 30 to 122 μm (*SI Appendix*, Fig. S1*H*). As in mouse, the majority of *NPPB*$^+$ neurons (94.5 ± 2.8%) coexpressed *CYSLTR2*, as well as a large proportion of *TRPV1*$^+$ neurons (76.3 ± 1.8%; Fig. 1 *H* and *I*). Overall, we found that *Cysltr2* was expressed in sensory neurons from both mice and humans that overlapped with *NPPB*, with a broader *CYSLTR2* expression in humans.

LTC_4 Specifically Induces Dose-Dependent Acute Itch. We next determined whether specific CysLTs induced itch when injected in vivo. Cheek injection of ligands into mice allows the distinguishing of pruritogens vs. algogens based on whether they trigger hind-paw scratching vs. nocifensive forepaw wiping behaviors, respectively (43) (Fig. 2*A*). For our behavioral analysis, we utilized an infrared behavior observation box (iBOB) in order to analyze scratching and wiping behaviors in the dark using infrared LEDs. We first injected the known ligands of $CysLT_2R$, LTC_4, or LTD_4. Because LTC_4 is rapidly converted to LTD_4 at the membrane, we used, in addition, a version of LTC4 conjugated with an N-methyl group ($NMLTC_4$), which is a nonhydrolyzable form resistant to conversion to LTD_4. We found that, while LTC_4 and $NMLTC_4$ cheek injections induced robust scratching behaviors, neither vehicle nor LTD_4 injections induced scratching (Fig. 2*B*). This was the case when quantified as total scratching bouts or duration of scratching (Fig. 2*B* and *SI Appendix*, Fig. S2*A*). LTC_4 and $NMLTC_4$ cheek injections did not induce wiping with the forepaws, indicative of pain (Fig. 2*C*). We next tested whether LTE_4, which is the terminal metabolite of the CysLT pathway, also had the ability to induce itch. We found that, while $NMLTC_4$ induced robust scratching behaviors, LTE_4 injections did not induce itch (Fig. 2*D*). Neither LTD_4 nor LTE_4 induced significant scratching or wiping behaviors over vehicle controls (Fig. 2 *B* and *D*). These data indicate that injections of LTC_4 and $NMLTC_4$, but not LTD_4 nor LTE_4, induced robust itch but not pain behaviors.

We next determined whether $NMLTC_4$ and LTC_4 induced a dose-dependent scratching response. LTC_4 and $NMLTC_4$ scratching curves had a bell shape, peaking at 0.2 to 0.6 nmol, whereas higher doses of LTC_4 and $NMLTC_4$ did not induce itch (Fig. 2 *F* and *G*). As pain can inhibit itch, we checked whether $NMLTC_4$ at higher doses could have a nociceptive effect; however, we detected no wiping indicative of pain (*SI Appendix*, Fig. S2*B*). LTD_4 did not induce scratching at any of the doses tested (Fig. 2*F*). The scratching induced by LTC_4 and $NMLTC_4$ occurred mainly during the first 30 min and is gone by 45 min (*SI Appendix*, Fig. S2*C*). Our phenotype was not affected by the infrared setup: $NMLTC_4$ induced itch that was similar when scored traditionally by observers in the light (Fig. 2*F*) as when

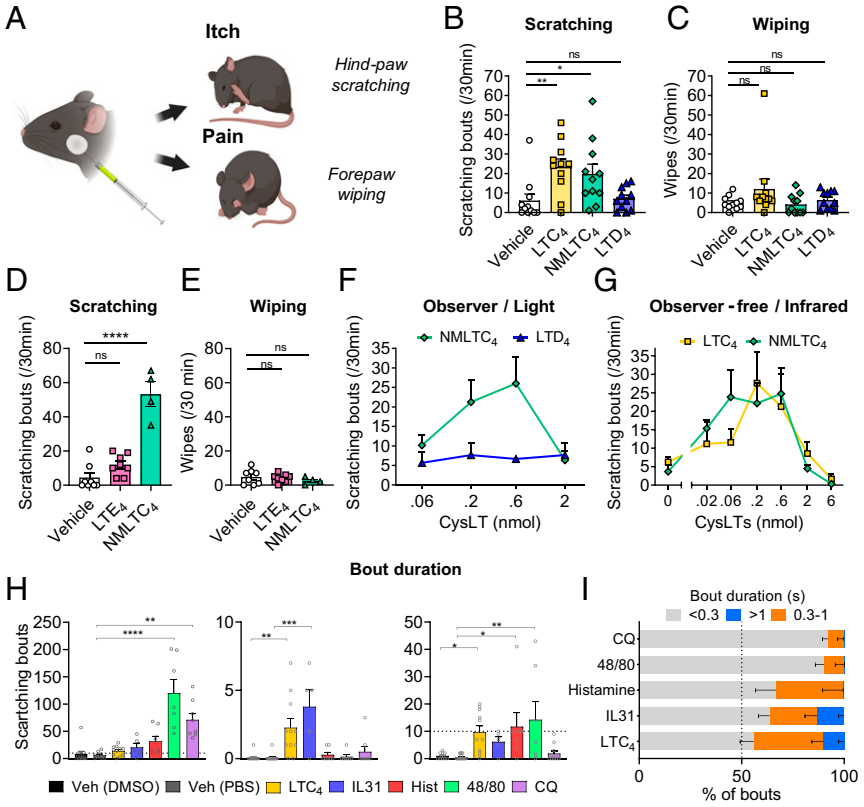

Fig. 2. LTC_4 but not LTD_4 or LTE_4 induces dose-dependent acute itch behaviors. (*A*) Diagram of experimental design of acute itch/pain induction by intradermal injection of ligands in the cheek of the mice. (*B*) Scratching bouts in response to vehicle, LTC_4, $NMLTC_4$, and LTD_4 at 0.6 nmol (n = 8 to 11). (*C*) Wiping responses, indicative of pain, to vehicle, LTC_4, $NMLTC_4$, and LTD_4 at 0.6 nmol (n = 8 to 11). (*D*) Scratching bouts in response to vehicle, $NMLTC_4$, and LTE_4 at 0.6 nmol (n = 4 to 8). (*E*) Wiping responses, indicative of pain, to vehicle, LTE_4, and $NMLTC_4$ at 0.6 nmol (n = 4 to 8). (*F*) Scratching bouts' dose responses to $NMTLC_4$ and LTD_4 were recorded for 30 min at different concentrations and scored live (n = 3 to 12). (*G*) Scratching bouts' dose responses to LTC_4 and $NMLTC_4$ were recorded for 30 min at different concentrations (n = 6 to 8). (*H* and *I*) Analysis of kinetics and scratching bout duration differences in response to various pruritogens: LTC_4 (0.6 nmol), IL-31 (0.02 nmol), histamine (100 μg), compound 48/80 (100 μg), CQ (200 μg), and vehicles (phosphate-buffered saline [PBS] and dimethyl sulfoxide [DMSO]). (*H*) Absolute numbers of bouts shorter than 0.3 s, bouts between 0.3 and 1 s, and bouts longer than 1 s. (*I*) Distribution of bouts according to their duration. Values presented as mean ± SEM. One-way ANOVA with Dunnett's posttest. ns, nonsignificant (*P < 0.05; **P < 0.01; ***P < 0.001; ****P < 0.0001).

recorded in iBOB (Fig. 2*G*). Therefore, LTC_4, but not LTD_4, gives a classic bell-shaped curve in dose dependency, which is similar to some other GPCR ligands, for acute itch induction.

LTC_4 Induces Itch that Is Distinct in Quality Compared with Other Itch Ligands. Most pruritogens have been classified based on their overall ability to induce itch, but the quality of the itch responses has not been well characterized. We next questioned whether scratching bouts induced by injections of different pruritogens could vary in kinetics or duration. We first looked at when itch occurred following intradermal cheek injections of several pruritogenic compounds: LTC_4 (0.6 nmol), IL-31 (0.02 nmol), histamine (100 μg), compound 48/80 (100 μg), and CQ (200 μg; Fig. 2 *H* and *I* and *SI Appendix*, Fig. S2*D*). IL-31, histamine, and CQ induce itch by acting directly on sensory neurons, while compound 48/80 triggers itch by activating MC through Mrgprb2 receptors (44).

We first measured the length of individual scratching bouts induced by pruritogens, and we empirically divided bouts in three categories: short bouts (<0.3 s), medium bouts (0.3 to 1 s), and long bouts (>1 s). By this analysis, LTC_4 induced a significant increase in medium and long bouts (Fig. 2*H*). Overall, 45% of bouts induced by LTC_4 were medium to long bouts (>0.3 s; Fig. 2*I*). By contrast, CQ and compound 48/80 induced a majority of shorter bouts, with less than 10% of longer bouts (>0.3 s; Fig. 2*I*). IL-31 showed a similar profile of scratching bouts as LTC_4, with a significant increase of long bouts and around 40% of medium-long bouts. Histamine produced a significant proportion of medium bouts but did not produce any long bouts (Fig. 2*H*). We observed that LTC_4-, CQ-, and histamine-induced itch started within the first 5 min, beginning at 4.1 min, 4.7 min, and 4.6 min on average, respectively (*SI Appendix*, Fig. S2*E*), while IL-31–induced itch started at 8.7 min and 48/80-induced itch started at 11.1 min (*SI Appendix*, Fig. S2*E*). LTC_4-induced itch is at the highest between 5 and 10 min (*SI Appendix*, Fig. S2*C*), while histamine-induced itch started and peaked at 10 min, CQ- and compound 48/80-induced itches started at 10 min and seemingly peaked at 15 to 20 min, whereas IL-31–induced itch was strongest at 25 to 30 min (*SI Appendix*, Fig. S2*F*).

Alloknesis is a form of itch that occurs when the skin gets sensitized by inflammatory mediators and responds to innocuous touch stimuli. For example, histamine injection induces strong alloknesis (45). The types of neurons involved and molecular mechanisms of alloknesis are different from acute ligand-induced itch (46). We asked whether LTC_4 was able to induce alloknesis following injection. The nape of the neck was injected by ligands, followed by stimulation with a thin Von Frey filament (*SI Appendix*, Fig. S2*G*). Histamine injection was able to increase the number of responses to that filament within 20 min (*SI Appendix*, Fig. S2*H*), and this alloknesis lasted until 3 h after injection (*SI Appendix*, Fig. S2*J*). However, LTC_4 did not induce sustained alloknesis during the first 60 min, nor at the 3 h time point (*SI Appendix*, Fig. S2 *H–J*). This shows that LTC_4 can induce acute scratching and itch but does not mediate alloknesis in naïve animals. These data, taken together, show that LTC_4 induces differences in kinetics and quality of itch following injection compared with other pruritogens.

LTC_4-Mediated Itch Is Dependent on $CysLT_2R$. We next determined the functional role of the $CysLT_2R$ receptor in CysLT-induced itch. In studies in the lung and also in heterologous systems, LTC_4 has been found to bind to both $CysLT_2R$ and $CysLT_1R$ with different affinities; therefore, it is important to clarify the roles of these receptors in vivo in itch. LTC_4-induced itch was significantly decreased in *Cysltr2*$^{-/-}$ mice compared with *Cysltr2*$^{+/+}$ control littermates (*SI Appendix*, Fig. S3 *A* and *B*). Levels of LTC_4-induced scratching in *Cysltr2*$^{-/-}$ mice did not appear to be completely gone (*SI Appendix*, Fig. S3*A*), so, to elucidate whether some residual itch was present, we repeated this experiment including a vehicle condition in wild-type (WT) mice as a comparison for baseline itch. We confirmed with this experiment that LTC_4-induced scratching was significantly decreased in *Cysltr2*$^{-/-}$ mice to levels compared with the vehicle condition (Fig. 3 *A* and *B*). $NMLTC_4$-induced itch was eliminated in *Cysltr2*$^{-/-}$ mice compared to *Cysltr2*$^{+/+}$ control littermates, indicating a major role for *Cysltr2* in mediating this itch (Fig. 3 *C* and *D*).

We next generated bone marrow (BM) chimeric mice to determine which cells expressing $CysLT_2R$ were involved in CysLT-induced itch, as the receptor is expressed on numerous immune cells in addition to sensory neurons. WT or *Cysltr2*$^{-/-}$ mice were lethally irradiated to eliminate radiosensitive hematopoietic cells but not somatic cells (including neurons), followed by transplantation with WT or *Cysltr2*$^{-/-}$ BM, thus reconstituting radiosensitive hematopoietic cells with WT or *Cysltr2*$^{-/-}$ genotypes (Fig. 3*E*). Flow cytometry of skin cells from BM-chimera mice showed that nearly 100% of eosinophils were from donor mice (*SI Appendix*, Fig. S4*B*), macrophages showed fractions from both donor and recipient origins (*SI Appendix*, Fig. S4*C*), and skin T cells were mostly from recipient mice (*SI Appendix*, Fig. S4*D*). These differences likely reflect the effect of radiation on proliferating vs. tissue-resident nondividing immune cells. Mice were injected with $NMLTC_4$ and scored for itch behavior. Irradiated *Cysltr2*$^{-/-}$ mice reconstituted with WT donor BM had lower levels of $NMLTC_4$-induced scratching compared with levels in naïve WT mice (Fig. 3*F*), whereas irradiated WT mice reconstituted from WT or *Cysltr2*$^{-/-}$ BM showed levels unchanged from naïve WT mice, indicating that *Cysltr2*-expressing radioresistant cells mediate $NMLTC_4$ itch (Fig. 3*F*).

We also investigated whether CysLTs acted through MCs to produce itch. MCs express *Cysltr2* (47) and generate LTC_4 during inflammation. MCs are major sources of histamine, serotonin, and other pruritogenic mediators that induce itch (41, 44). MCs are radioresistant and would not be affected in BM chimeras (48). We found that $NMLTC_4$ induced equivalent itch in *Kit*$^{Wsh/Wsh}$ mice deficient for MCs as their WT littermates (Fig. 3*G*).

We next asked whether $CysLT_1R$ was involved in CysLT-induced itch. When injected with $NMLTC_4$, *Cysltr1*$^{-/-}$ mice had the same levels of scratching as their *Cysltr1*$^{+/+}$ littermates (Fig. 3*H*). These data indicate that $CysLT_2R$ but not $CysLT_1R$ is involved in CysLT-induced itch. TRP channels are known to be activated and induce calcium influxes downstream of GPCRs in itch pathways. TrpV1 mediates histamine-dependent neuronal signaling and itch (26), while TrpA1 mediates CQ or BAM8-11 scratching through MrgprA1 and MrgprC11, respectively (49). As most *Cysltr2*$^{+}$ neurons expressed *Trpv1* (Fig. 1*E* and *SI Appendix*, Fig. S1 *A* and *B*) and *Trpa1* (*SI Appendix*, Fig. S1*B*), we next determined whether CysLT responses could also be mediated through those TRP channels. We first found that $NMLTC_4$-induced and LTC_4-induced itch was not altered in *Trpv1*$^{-/-}$ mice (Fig. 3*I* and *SI Appendix*, Fig. S3*C*). We then found that preinjecting the TrpA1 antagonist HC-030031 in the cheek failed to inhibit $NMLTC_4$-induced scratching (*SI Appendix*, Fig. S3*D*). These data indicate that targeting TrpV1 or TrpA1 alone is unable to impact LTC_4-induced itch. Taken together, these results show that LTC_4 can induce itch in mice by acting through $CysLT_2R$ in nonhematopoietic cells and in a manner independent from MC, $CysLT_1R$, and TrpV1.

We next asked if there could be interactions between the CysLTs in itch. LTD_4, which we found does not induce itch when injected acutely (Fig. 2 *B* and *F*), inhibited $NMLTC_4$-induced itch when coinjected with $NMLTC_4$ (Fig. 3*J*). LTD_4 is able to act through both $CysLT_1R$ and $CysLT_2R$, so we tested whether this inhibition was dependent on $CysLT_1R$ expression. Interestingly, LTD_4 inhibition of $NMLTC_4$-induced itch was intact in *Cysltr1*$^{-/-}$

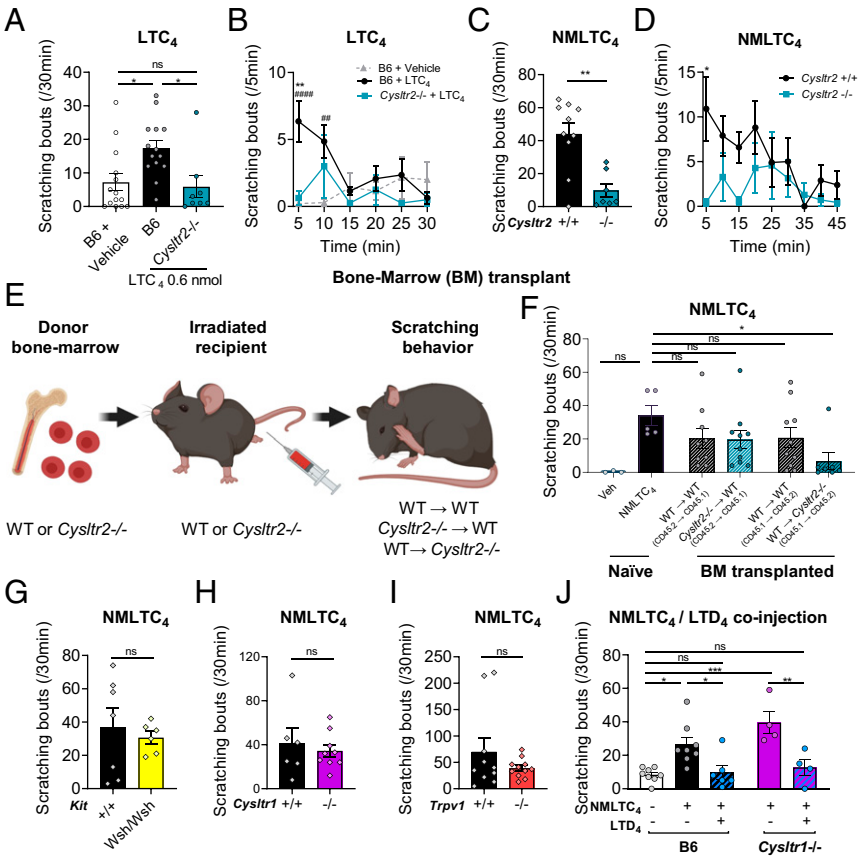

Fig. 3. LTC_4-induced itch is dependent on $CysLT_2R$. (*A* and *B*) Scratching bouts induced by intradermal cheek injection of vehicle or LTC_4 0.6 nmol in B6 mice or by injection of LTC_4 0.6 nmol in *Cysltr2*$^{-/-}$ mice (7 to 44 wk old; *A*) and detailed scratching bout kinetics over 30 min ($^{\#}$B6 + LTC_4 vs. B6 + vehicle; *B6 + LTC_4 vs. *Cysltr2*$^{-/-}$ + LTC_4; *B*). (*C* and *D*) Scratching bouts induced by intradermal cheek injection in *Cysltr2*$^{+/+}$ or *Cysltr2*$^{-/-}$ mice of $NMLTC_4$ (0.6 nmol; *C*) and detailed scratching bout kinetics over 45 min (*D*). (*E* and *F*) Generation of BM chimeras with WT or *Cysltr2*$^{-/-}$ mice as donors and WT or *Cysltr2*$^{-/-}$ mice as recipients. (*E*) Diagram of BM transplant procedure. (*F*) Scratching bouts induced by intradermal cheek injection of $NMLTC_4$ 0.6 nmol in naïve mice and in BM chimera. Behavior recorded in daylight settings (not in iBOB). (*G–I*) Scratching bouts induced by intradermal cheek injection of $NMLTC_4$ (0.6 nmol) in (*G*) *Kit*$^{Wsh/Wsh}$ mice, (*H*) *Cysltr1*$^{-/-}$ mice, and (*I*) *Trpv1*$^{-/-}$ mice. (*J*) Scratching bouts induced by the coinjection of $NMLTC_4$ (0.6 nmol) and LTD_4 (2 nmol) in B6 mice and in *Cysltr1*$^{-/-}$ mice. Values presented as mean ± SEM. Unpaired *t* test (*C*, *G*, and *I*), repeated-measures two-way ANOVA with Šidák's posttest (*B* and *D*), one-way ANOVA with Dunnett's posttest (*F*), and one-way ANOVA with Tukey's posttest (*A* and *J*). ns, nonsignificant (*$P < 0.05$; **$P < 0.01$; ***$P < 0.001$).

mice (Fig. 3*J*), showing that this inhibition is independent of $CysLT_1R$ and suggesting a potential competitive antagonism at $CysLT_2R$.

$CysLT_2R$ Does Not Mediate Dry Skin or *Alternaria*-Induced Itch. We next wished to determine whether $CysLT_2R$ plays an endogenous role in physiological models of skin pathology and itch. *Cysltr2*$^{-/-}$ mice did not have a defect in histamine-induced itch (*SI Appendix*, Fig. S5*A*). Similarly, the MC degranulator compound 48/80 induced robust scratching that was not reduced in *Cysltr2*$^{-/-}$ mice (*SI Appendix*, Fig. S5*B*). *Alternaria alternata* is an environmental airborne fungus involved in allergic diseases like asthma and potentially AD. It has recently been shown to be able to induce acute itch and scratching when injected intradermally (50). We show here that *Alternaria*-induced itch was $CysLT_2R$-independent (*SI Appendix*, Fig. S5 *C–E*). Dry skin is a major cause of itch (51), and dry skin-induced itch can be modeled in mice by repeated application of a mixture of acetone and ether followed by water (AEW) for 5 d (*SI Appendix*, Fig. S5*F*). We found that AEW-induced itch and scratching behaviors were equivalent in *Cysltr2*$^{-/-}$ mice as compared with littermate controls (*SI Appendix*, Fig. S5*H*). Taken together, these data show that $CysLT_2R$ does not mediate dry skin or *Alternaria*-induced itch.

CysLT Pathway and $CysLT_2R$ in a Model of Chronic Itch. We next investigated the role of the endogenous CysLT pathway in chronic itch and dermatitis and utilized the MC903 model of skin inflammation, which has some characteristics of AD and ACD (52). The vitamin D analog MC903 induces skin thickening, immune cell influx, inflammation, and itch (29, 53). When we applied MC903 to the ears of male and female mice over 12 d (Fig. 4*A*), we found that this treatment caused spontaneous scratching behaviors (Fig. 4*B*), thickening of the ear (Fig. 4*C*), and severe acanthosis (thickening of epidermis), hyperkeratosis (thickening of the stratum corneum), and inflammation (Fig. 4*D* and *SI Appendix*, Fig. S6*A*). Flow cytometry analysis of the ear skin revealed a major influx of immune cells, including eosinophils, neutrophils, dendritic cells, macrophages, and T cells detectable at day 6 and with a peak at day 12 (*SI Appendix*, Fig. S6 *B* and *C*). Staining with toluidine blue at day 12 revealed an increase in the MC number present in the ear (*SI Appendix*, Fig. S7 *A* and *B*). However, we found that MCs were unlikely to be involved in driving chronic itch or skin inflammation in this model: WT controls and *Kit*$^{Wsh/Wsh}$ mice deficient in MCs showed similar levels of itch behavior and ear thickening (*SI Appendix*, Fig. S7 *C* and *D*). We next determined the role of *Trpv1*$^{+}$ neurons in MC903-induced itch, given that *Trpv1* expression encompasses *Cysltr2* expression in the DRG. Using resiniferatoxin (RTX) to ablate *Trpv1*$^{+}$ neurons, we observed that

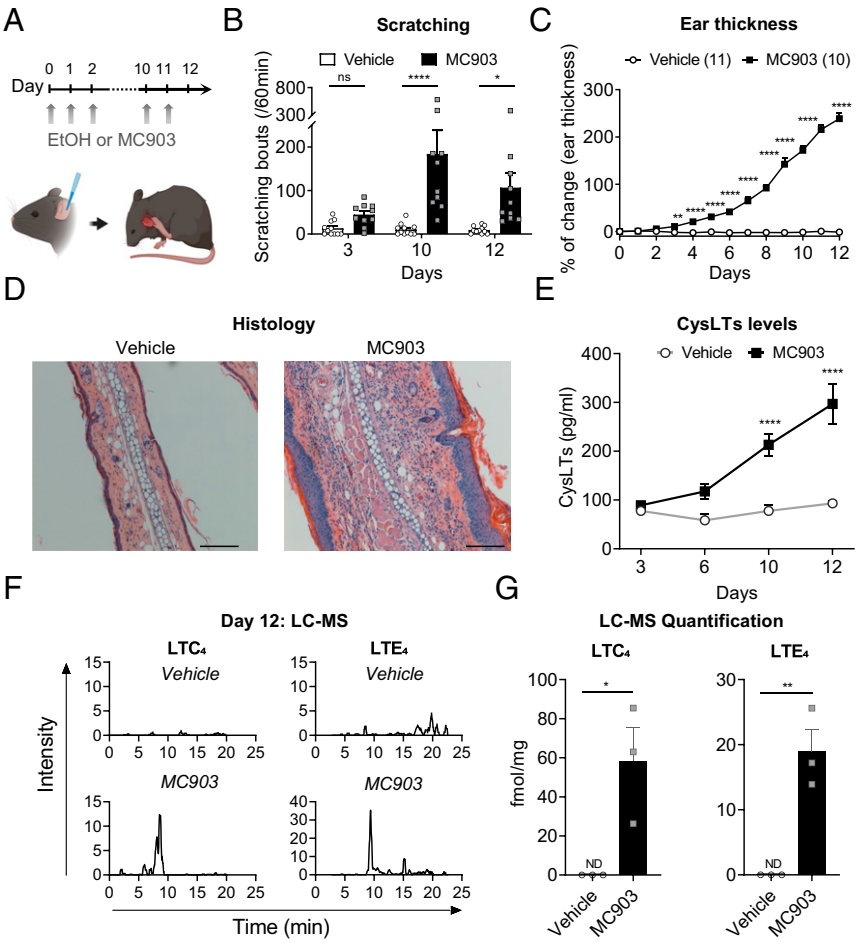

Fig. 4. CysLT levels are increased in the skin of the MC903 model of dermatitis and itch. (*A*) Diagram of procedure: daily application of MC903 on the mouse ear for 12 d. (*B*) Scratching bouts recorded on days 3, 10, and 12 for 60 min before daily application of vehicle (ethanol) or MC903. (*C*) Percentage of ear thickness change following daily application of vehicle or MC903. (*D*) H&E staining performed on ear section at day 12 of MC903 model. (Scale bar: 50 μm.) (*E*) CysLTs (LTC_4, LTD_4, and LTE_4) levels measured by ELISA at days 3, 6, 10, and 12 (n = 5 to 6). (*F* and *G*) Liquid chromatography–mass spectrometry. (*F*) Representative chromatograms for LTC_4 (*Left*) and LTE_4 (*Right*) from ear homogenates at day 12 after daily vehicle treatment (*Top*) or MC903 treatment (*Bottom*). (*G*) LTC_4 and LTE_4 quantification per milligram of ear collected at day 12 after vehicle or MC903 treatment. Values presented as mean ± SEM. Repeated-measures two-way ANOVA, Šidák's posttest (*B* and *C*), two-way ANOVA with Šidák's posttest (*E*), and unpaired t test (*G*). ns, nonsignificant (*$P < 0.05$; **$P < 0.01$; ***$P < 0.001$; ****$P < 0.0001$).

RTX-treated mice failed to develop any itch/scratching behaviors in response to MC903 treatment (*SI Appendix*, Fig. S8*A*) while showing the same levels of ear thickening as control mice (*SI Appendix*, Fig. S8*B*), indicating that these neurons do mediate itch but not overall inflammation in this model.

We next investigated whether CysLTs and $CysLT_2R$ played a role in the MC903 model. Given that many immune cells recruited into the skin, including eosinophils, MCs, and dendritic cells, can generate CysLTs, we hypothesized that we could detect an increase in these key lipid mediators. Using enzyme-linked immunoassays (ELISAs), we first measured the overall CysLT levels from skin homogenates. CysLTs steadily increased over time, with significant differences at day 10 and day 12 (Fig. 4*E*). We next used mass spectrometry to detect individual CysLTs (LTC_4, LTD_4, and LTE4) in ear homogenates at day 12. While MC903-inflammed ears had significant levels of LTC_4 and LTE_4, none were detectable in the vehicle conditions. LTC_4 in particular was highly elevated in MC903 samples, with LTE_4 detected at lower levels and levels of LTD_4 too low to be reliably measured (Fig. 4 *F* and *G*). Therefore, CysLTs are significantly induced in MC903-inflamed ears, with the highest level of LTC_4 at the later stage of inflammation.

We next ascertained the role for $CysLT_2R$ in this model of skin inflammation and itch. We found that MC903-treated *Cysltr2*$^{-/-}$ mice had similar scratching levels as wild-type control littermates at early time points of the model; however, at day 12, *Cysltr2*$^{-/-}$ mice showed a significant decrease in scratching compared with WT controls (Fig. 5*A*). Our findings do indicate, therefore, a specific role for $CysLT_2R$ in later phases of itch in this model. Previous work had shown contributions of other major mediators to earlier phases of MC903-induced itch, such as neutrophils and CXCL10, which were more involved before day 10 (54). Analysis of bout duration at the day 12 timepoint further showed that the decrease in scratching in *Cysltr2*$^{-/-}$ mice was observed in both short bouts (<0.3 s) and longer bouts, with a significant decrease in long bouts (>1 s) in the *Cysltr2*$^{-/-}$ mice (Fig. 5*B*).

We next determined whether $CysLT_2R$ mediates skin inflammation in MC903-treated mice, given its known role in ovalbumin-induced skin thickening and collagen deposition in a different model of dermatitis (14). Interestingly, we found no difference between *Cysltr2*$^{-/-}$ and littermate controls in ear swelling over time (Fig. 5*C*) or in epidermal thickening as analyzed by hematoxylin and eosin (H&E) staining (Fig. 5 *D* and *E*). However, we

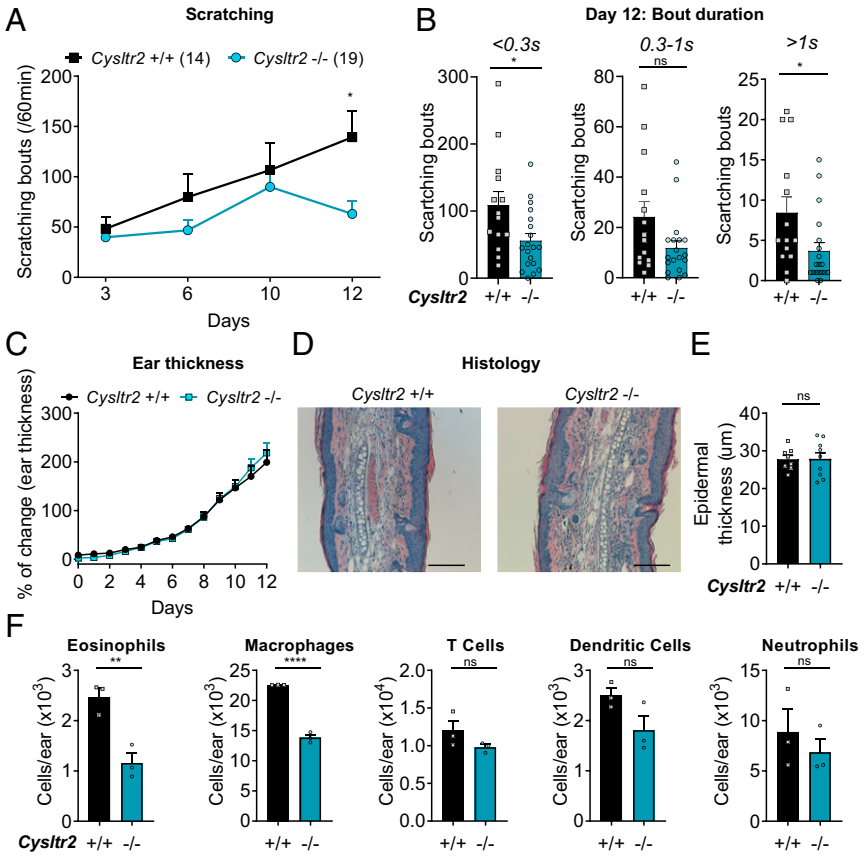

Fig. 5. CysLT$_2$R is involved in chronic itch but not in inflammation in MC903. (*A*) Scratching bouts recorded on days 3, 6, 10, and 12 for 60 min before daily application of MC903 in *Cysltr2*$^{+/+}$ or *Cysltr2*$^{-/-}$ mice. (*B*) Bout duration analysis for *Cysltr2*$^{+/+}$ and *Cysltr2*$^{-/-}$ mice at day 12 of MC903 (number of bouts: <0.3 s, between 0.3 and 1 s, and >1 s). (*C*) Percentage of ear thickness change following daily application of MC903 in *Cysltr2*$^{+/+}$ or *Cysltr2*$^{-/-}$ mice. (*D* and *E*) H&E staining performed on ear section at day 12 of the MC903 model in *Cysltr2*$^{+/+}$ or *Cysltr2*$^{-/-}$ mice. (*D*) Representative images of H&E staining. (*E*) Quantification of epidermal thickness (n = 8 to 9 with 10 to 15 fields quantified per animal). (*F*) Quantification of immune cell populations by flow cytometry from ear homogenates collected at day 12 from *Cysltr2*$^{+/+}$ or *Cysltr2*$^{-/-}$ mice (n = 3). Values presented as mean ± SEM. Repeated-measures two-way ANOVA, Šidák's posttest (*A* and *C*), and unpaired t test (*B*, *E*, and *F*). ns, nonsignificant (*P < 0.05; **P < 0.01; ****P < 0.0001).

did find, by flow cytometry analysis, significant decreases in some specific immune cells, including eosinophils and macrophages, in the skin of *Cysltr2*$^{-/-}$ mice at day 12, while T cells, dendritic cells, and neutrophils remained unchanged (Fig. 5*F*).

As a comparison with *Cysltr2*$^{-/-}$ mice, we next determined that the increase in ear thickness and itch behaviors were not impaired in *Cysltr1*$^{-/-}$ mice in the MC903 model (*SI Appendix*, Fig. S9), indicating that CysLT$_1$R is not involved in mediating chronic itch. These data, taken together, indicate that CysLT$_2$R specifically contributes to itch in the late stage of inflammation in MC903-treated mice.

Discussion

Chronic itch negatively impacts the quality of life in patients with AD and ACD. Recent advances in the field have highlighted the importance of molecular receptors for immune mediators and neuroimmune cross-talk in those processes (29, 54, 55). CysLTs have long been suspected to be an important mediator of allergic skin reactions. CysLTs produce wheal and flare reactions when injected into human skin (56). LTC$_4$ is released in great quantities during in vivo allergic cutaneous reactions to ragweed or grass pollen antigen (57), and LTC$_4$ levels are increased in the skin of patients with AD (58). The presence of *Cysltr2* expressed by the NP3 subset of pruriceptors strongly hinted at a role for the CysLTs/CysLT$_2$R pathway in itch, but its functional relevance had not been explored prior to this study. Our study definitively shows that LTC$_4$, but no other CysLTs, can specifically and functionally induce itch in vivo through the CysLT$_2$R receptor, and that CysLT$_2$R contributes to itch in a physiological model of dermatitis.

Prior to our work, two previous studies have suggested a potential role of NMLTC$_4$ and LTD$_4$ in inducing itch (31, 41). In a first study, LTD$_4$ was injected intradermally at one dose and found to induce itch similarly to serotonin and IL-31 (31). By contrast, we found that LTD$_4$ does not produce itch in a detailed dose–response analysis. A more recent study found that NMLTC$_4$ induced calcium influx into mouse DRG neurons and induced itch following acute injections in mice at one dose, together with sphingosine 1 phosphate and serotonin (41). While this did show initial phenotypes induced by NMLTC$_4$ with scratching behaviors, without a comparison with endogenous LTC$_4$ or other CysLTs, the physiological relevance of this response in inflammatory itch and the role of CysLT$_2$R in both acute and chronic itch remained unknown.

Here, we show that LTC$_4$, in particular, is a critical mediator of itch, and that CysLT$_2$R mediates this functional response in vivo in acute LTC$_4$-induced itch, and also is relevant in a chronic model of itch. Even though CysLT$_2$R expressed in heterologous cell systems binds to both LTC$_4$ and LTD$_4$ in vitro (10), in vivo datasets show a more context-dependent role of each ligand in how it interacts with the receptor. CysLT$_2$R is preferentially activated by LTC$_4$ in vivo in platelets (13) and

during type 2 airway immunopathology (19). Our data on itch fits with LTC_4 and not LTD_4 in being the major driver of itch in vivo. We found that LTD_4 was able to inhibit $NMLTC_4$ itch when it was coinjected with $NMLTC_4$. Previous work has shown that LTC_4/$CysLT_2R$ and LTD_4/$CysLT_1R$ pathways can have antagonistic effects: $CysLT_2R$ negatively regulates $CysLT_1R$-dependent Th2 pulmonary inflammation to dust mites in mice sensitized and challenged with *Dermatophagoides farinae* (11) and $CysLT_1R$-induced mitogenic signaling responses of MC (59). However, in our study, LTD_4 inhibition of $NMLTC_4$-induced scratching was still present in *Cysltr1*$^{-/-}$ mice, showing that the mechanism was $CysLT_1R$-independent. A recent study in platelet biology indicates interesting parallels with our data (60). In this study, it was shown that LTD_4 inhibits LTC_4-driven platelet activation in vitro in a manner independent of $CysLT_1R$, most likely by the ligand competing with LTC_4 on the $CysLT_2R$ receptor (60).

We found that, while LTC_4 and $NMLTC_4$ induce increasing itch at lower doses, this response no longer occurred at high doses. The bell-shaped curve observed with LTC_4 and $NMLTC_4$ may be similar to other pruritogen responses, such as the inverted U-shaped itch response observed with CQ injections (61). Given that many of the pruritogen receptors are membrane-bound GPCRs, it could be related to receptor internalization and desensitization. $CysLT_1R$ receptors are known to undergo rapid agonist-dependent internalization (62, 63). A recent study found that a high dose of LTC_4 induced internalization of $CysLT_2R$ in MCs, while a low dose induced its expression at the membrane (64). The downstream signaling of $CysLT_2R$ in neurons is yet unknown. Our results show that TrpV1, which mediates histamine-dependent neuronal signaling and itch (26), was unnecessary for LTC_4-induced itch. Our data also do not indicate a role for TrpA1, which is involved in itch dependent on MrgprA3 and MrgprC11 (49). Nonetheless, it is possible that double deficiency in both ion channels could show a phenotype, and this remains to be determined with further studies.

Other than sensory neurons, many other cell types express $CysLT_2R$, including myeloid immune cells (3). By using BM chimeras from *Cysltr2*$^{-/-}$ mice, our results showed that receptor expression in radiosensitive hematopoietic cells such as eosinophils was unnecessary for $NMLTC_4$-induced itch, while *Cysltr2* in radioresistant cells was necessary. These data fit with a role for *Cysltr2* in sensory neurons, which are radioresistant nonhematopoietic cells. Future studies using conditional knockout mice for *Cysltr2* are necessary to determine its exact role in neurons.

We also investigated the kinetics and the quality of itching induced by distinct ligands, finding that LTC_4-induced scratching differed from histamine, CQ, and compound 48/80 by having longer bouts. Potentially, the responsive neuronal subset could determine the subsequent itch responses. LTC_4 and IL-31, which are ligands for $CysLT_2R$ and IL-31ra coexpressed by NP3 neurons, induce the same type of longer scratching bouts. CQ, which activates MrgprA3 expressed on NP2 neurons, produces almost exclusively short bouts. Histamine receptors are known to be spread across NP3 and NP2 subsets (32), which could explain the intermediary phenotype observed with histamine. Furthermore, LTC_4 did not induce alloknesis (touch-induced itch). While chemical ligands can be coupled to itch by direct gating of pruriceptors, alloknesis is processed by other sensory neurons, including TLR5-expressing Aβ low-threshold mechanoreceptors (reviewed in ref. 46).

Transcript types and expression levels in DRG neurons can differ significantly between different species (65). We showed here that the expression of the Cysltr2 transcript was broader in human DRG neurons (63%) than in mouse DRG neurons (10%). Most neurons expressing *NPPB* coexpressed *CYLTR2* in human neurons; however, *CYLTR2* expression was not limited to *NPPB*$^{+}$ neurons. The broader CYLTR2 expression in human DRG neurons suggests that the receptor is relevant to human sensory physiology and might have roles beyond those we have highlighted in the mouse. A recent study highlighted the differences between mouse and human sensory neurons, including Trpv1 expression (~30% in mice vs. ~70% in humans) and TSLP receptor expression (~70% in mice vs. ~5% in humans) (66). In rats, a previous study found that *Cysltr2* was expressed in 36% of DRG neurons and that $CysLT_2R$ could be involved in mediating pain in rats (67). *Cysltr2*$^{+}$ rat neurons were mainly isolectin B4^{+} neurons coexpressing ATP receptor *P2rx3*, and LTC_4 injected into the footpad of rats potentiates αβ-me-ATP–induced thermal hyperalgesia (67). This contrasts with mouse DRG neurons, where *Cysltr2* is expressed in ~10% of sensory neurons and *P2rx3* is in a much broader population of neurons (31, 32, 41). In our study, we did not find nocifensive phenotypes with LTC_4 cheek injections, which does not rule out sensitization of pain, but shows no induction of acute pain phenotypes. Another study found that sensory neurons from the trigeminal ganglion innervating the nasal mucosa of guinea pigs expressed *Cysltr1* rather than *Cysltr2*, and LTD_4 could increase the excitability of those neurons (68). By contrast, we do not detect *Cysltr1* transcript in mouse DRG neurons and do not find a functional role for $CysLT_1R$ in itch. These distinct findings in human, mouse, rat, and guinea pigs highlight a need for species-specific analysis of sensory transcripts, and may have implications for translatability of results from mouse to humans in itch biology.

We demonstrated the involvement of the CysLT pathway and $CysLT_2R$ in the MC903 mouse model of chronic itch. In this mouse model of dermatitis, several immune and inflammatory mediators have been found to contribute to chronic itch. The cytokines TSLP, IL-4, and IL-13, as well as serotonin and its receptor 5HTR7, have been found to critically drive itch in this model (29, 52–54). Recent work has shown that neutrophils and the chemokine CXCL10 mediate distinct phases of inflammation and itch in MC903 mice (54). Interestingly, this study showed that *Cysltr2*, *Nppb*, and *Il31ra* are transcriptionally up-regulated in trigeminal neurons following cheek application of MC903 (days 5 to 8). We found that CysLT levels went up in the skin especially in the later stages of the MC903 model. The detection of LTC_4 at day 12 indicates that the production of CysLTs is actively ongoing at that stage, since LTC_4 is quickly converted to LTD_4 (69), and it is at day 12 that *Cysltr2*$^{-/-}$ mice showed a significant decrease in itch, suggesting that active LTC_4 production at that stage is able to induce scratching. Future studies are needed to determine how $CysLT_2R$ signaling synergizes with the other cytokine- and immune cell-driven pathways in this model to drive itch signaling.

We found that several immune cell types increased in MC903-treated mice, which could be sources of CysLTs. In the skin and other tissues, CysLTs are produced by eosinophils, MC, macrophages, and monocytes (70, 71). MCs generate CysLTs upon activation (72) and communicate with neurons bidirectionally in inflammation and itch (73). However, we observed that mice lacking MC (*Kit*$^{Wsh/Wsh}$) showed intact itch in MC903-treated mice. Eosinophils are other possible candidates. Eosinophil-derived LTC_4 acts on fibroblasts through $CysLT_2R$ to induce collagen deposition and skin thickening in ovalbumin-induced allergic sensitization (14). Macrophages and dendritic cells are also high expressers of LTC_4S, which is the enzyme that produces LTC_4 (Immgen database; https://www.immgen.org/). Of note, we found that both eosinophils and macrophages decreased in *Cysltr2*$^{-/-}$ mice after MC903 challenge. Therefore, LTC_4 might be acting through both immune cells and sensory neurons to drive itch in vivo, and the relative roles of sensory neuron-expressed $CysLT_2R$ compared with nonneuronal $CysLT_2R$ in the MC903 model remain to be determined. It is possible that there is a positive neuroimmune feedback loop between CysLT-induced itch and immune cell recruitment through $CysLT_2R$.

By contrast with the MC903 model, we did not find a role for $CysLT_2R$ in the *Alternaria* model or compound 48/80-induced itch. $CysLT_2R$ also did not mediate AEW model of dry skin itch. One major difference between MC903 and the AEW models is that AEW does not cause significant infiltration of inflammatory cells in the dermis (74). *Alternaria* and compound 48/80 are both acute inflammatory models that could drive other immune pathways and cellular recruitment distinct from MC903-driven skin immune responses.

Our study may have therapeutic implications for treatment of dermatitis. The 5-LO inhibitor zileuton, which targets upstream conversion of arachidonic acid to LTA_4, has demonstrated efficacy in treating pruritus in small clinical trials (75). The $CysLT_1R$-specific antagonist montelukast (Singulair), which is successful in treating bronchoconstriction in asthmatic patients (9, 17), was tested in the treatment of AD patients but showed mixed results (76–79). Our work indicates that montelukast might have failed to show positive results because it targets $CysLT_1R$ instead of $CysLT_2R$.

The role of the CysLT pathway and its receptors in skin conditions has been suspected for a long time but has not been previously studied in itch. Here, we have shown that LTC_4, acting through $CysLT_2R$, is able to induce scratching in mice and participated in chronic itch in a mouse model of AD. This suggests that drugs targeting $CysLT_2R$ could be useful to treat recalcitrant chronic itch.

Materials and Methods

Detailed descriptions of methods and materials are provided in *SI Appendix, Materials and Methods*.

Mice. All animal experiments were approved by the Harvard Medical School Institutional Animal Care and Use Committee.

BM Chimera Generation. BM was collected from tibia, femur, and hips of both sides of either WT (C57BL/6) or *Cysltr2*$^{-/-}$ mice 8 to 12 wk of age, dissected and cleaned from all soft tissue. Recipient animals (WT or *Cysltr2*$^{-/-}$) 6 to 12 wk of age underwent lethal irradiation on the day of the transplantation. At 3 to 5 h after lethal irradiation, mice were anesthetized with isoflurane for retrobulbar injection of 3×10^6 BM donor cells. After 6 to 8 wk, behavioral experiments were performed.

Mouse RNAscope In Situ Hybridization Analysis. DRGs were dissected from mice and embedded in optimal cutting temperature compound, and cryosections of 16 μm were cut. Multilabeling in situ hybridization (ISH) was performed using the RNAscope technology (ACD) according to the manufacturer's instructions. Probes against mouse *Cysltr2*, *Trpv1*, *Nppb*, *Mrgpra3*, *Mrgprd*, *Hrh1*, *Tubb3*, and *Scn10a* in conjunction with the RNAscope multiplex fluorescent development kit were used.

Human DRG RNAscope Analysis. Procurement procedures for all human tissue were approved by the institutional review board at the University of Texas at Dallas, and samples were deidentified prior to use in the study. Human lumbar dorsal root ganglions collection and RNAscope in situ hybridization were performed as described previously (66).

Behavioral Analysis. For all behavior experiments, experimenters were blinded to experimental groups and/or genotypes. Recording of behaviors was performed with an experimental setup that enables us to record the mice in the dark in an experimenter-free environment: iBOB (Crimson Scientific) unless otherwise specified. Acute itch and pain behavior experiments were performed as described previously (43).

Bout duration quantification. Duration of individual bouts was measured, and bouts were then classified in three categories according to their length: <0.3 s, 0.3 to 1 s, and 1 s.

Touch-induced itch (alloknesis). For touch-induced itch, the nape of neck was mechanically stimulated using a 0.07-g Von Frey filament for 1 s three times in a row, with this sequence repeated three times, and the scratching responses was recorded out of a total of nine.

Chronic itch models. The MC903 model of chronic itch was performed as described previously (29, 53), and dry skin-evoked itch behaviors assessment was carried out as previously described (80).

Cysteinyl LT Detection. Whole ears from mice were collected, and CysLT generation was measured in acetone-precipitated homogenates by a commercially available ELISA according to the manufacturer's protocol (Cayman).

Mass Spectrometry. Samples were analyzed on an ultimate 3000 LC coupled with a Q Exactive plus mass spectrometer (Thermo Fisher), with a method based on previous studies (81, 82).

Flow Cytometry. Ears were mechanically separated and minced, then digested. The preparation was stained with antibodies. Flow cytometry was conducted on an LSRII flow cytometer.

Statistics Analysis. Data in figures represent mean ± SEM. All significance tests were chosen considering the experimental design, and we assumed normal distribution and variance of data. No data were excluded from statistical analyses unless due to technical errors. Statistical significance was determined by unpaired Student's *t* test for two-group comparisons, one-way ANOVA, or ANOVA for multivariate linear models. Statistical analyses were performed using Prism 7 (GraphPad Software).

Data Availability. All study data are included in the article and/or supporting information.

ACKNOWLEDGMENTS. We thank members of the I.M.C. laboratory, especially Nicole J. Yang and Kimbria Blake, for helpful discussions. We thank James Searson, Lin Ni, Amélie Bouvier, Noah Gilman, Victoria Flecha Maria, Tsz Man Fion, Lucy Wesemann, and Samantha Choi for strong technical support and watching behavioral videos. We thank Mark A. Hoon, Hans J. Solinski, and Juan-Manuel Leyva-Castillo for sharing their technical expertise and advice on neurobiological and immunological analysis. We are grateful to the Microscopy Resources on the North Quad core at Harvard Medical School and the Harvard Center for Mass Spectrometry for excellent technical assistance. Schematic diagrams were created using BioRender. Research in the I.M.C. laboratory is supported by NIH Grants (DP2AT009499, R01AI130019), the Food Allergy Science Initiative, GlaxoSmithKline and Allergan Pharmaceuticals, the Harvard Stem Cell Institute, and the Burroughs Wellcome Fund. This work was also supported by the Brigham and Women's Hospital Hypersensitivity Fund (to K.F.A.), National Institutes of Allergy and Infectious Diseases Grant K08 AI132723 (to L.G.B.), and the American Academy of Allergy, Asthma & Immunology Foundation Faculty Development Award (to L.G.B.). Research in the T.J.P. laboratory is supported by the NIH Grant (NS111929).

1. X. Dong, X. Dong, Peripheral and central mechanisms of itch. *Neuron* **98**, 482–494 (2018).
2. M. A. Hoon, Molecular dissection of itch. *Curr. Opin. Neurobiol.* **34**, 61–66 (2015).
3. Y. Kanaoka, K. F. Austen, Roles of cysteinyl leukotrienes and their receptors in immune cell-related functions. *Adv. Immunol.* **142**, 65–84 (2019).
4. T. M. Laidlaw *et al*., Cysteinyl leukotriene overproduction in aspirin-exacerbated respiratory disease is driven by platelet-adherent leukocytes. *Blood* **119**, 3790–3798 (2012).
5. S. Ualiyeva *et al*., Airway brush cells generate cysteinyl leukotrienes through the ATP sensor P2Y2. *Sci. Immunol.* **5**, eaax7224 (2020).
6. B. K. Lam, K. F. Austen, Leukotriene C4 synthase: A pivotal enzyme in cellular biosynthesis of the cysteinyl leukotrienes. *Prostaglandins Other Lipid Mediat.* **68-69**, 511–520 (2002).
7. Y. Kanaoka, A. Maekawa, K. F. Austen, Identification of GPR99 protein as a potential third cysteinyl leukotriene receptor with a preference for leukotriene E4 ligand. *J. Biol. Chem.* **288**, 10967–10972 (2013).
8. L. G. Bankova *et al*., Leukotriene E4 elicits respiratory epithelial cell mucin release through the G-protein-coupled receptor, GPR99. *Proc. Natl. Acad. Sci. U.S.A.* **113**, 6242–6247 (2016).
9. K. R. Lynch *et al*., Characterization of the human cysteinyl leukotriene CysLT1 receptor. *Nature* **399**, 789–793 (1999).
10. C. E. Heise *et al*., Characterization of the human cysteinyl leukotriene 2 receptor. *J. Biol. Chem.* **275**, 30531–30536 (2000).
11. N. A. Barrett *et al*., Cysteinyl leukotriene 2 receptor on dendritic cells negatively regulates ligand-dependent allergic pulmonary inflammation. *J. Immunol.* **189**, 4556–4565 (2012).
12. N. A. Barrett *et al*., Dectin-2 mediates Th2 immunity through the generation of cysteinyl leukotrienes. *J. Exp. Med.* **208**, 593–604 (2011).
13. H. E. Cummings *et al*., Cutting edge: Leukotriene C4 activates mouse platelets in plasma exclusively through the type 2 cysteinyl leukotriene receptor. *J. Immunol.* **191**, 5807–5810 (2013).

14. M. K. Oyoshi *et al*., Eosinophil-derived leukotriene C4 signals via type 2 cysteinyl leukotriene receptor to promote skin fibrosis in a mouse model of atopic dermatitis. *Proc. Natl. Acad. Sci. U.S.A.* **109**, 4992–4997 (2012).
15. T. A. Doherty *et al*., Lung type 2 innate lymphoid cells express cysteinyl leukotriene receptor 1, which regulates TH2 cytokine production. *J. Allergy Clin. Immunol.* **132**, 205–213 (2013).
16. J. von Moltke *et al*., Leukotrienes provide an NFAT-dependent signal that synergizes with IL-33 to activate ILC2s. *J. Exp. Med.* **214**, 27–37 (2017).
17. B. Volovitz *et al*., Montelukast, a leukotriene receptor antagonist, reduces the concentration of leukotrienes in the respiratory tract of children with persistent asthma. *J. Allergy Clin. Immunol.* **104**, 1162–1167 (1999).
18. H. P. Zhang, C. E. Jia, Y. Lv, P. G. Gibson, G. Wang, Montelukast for prevention and treatment of asthma exacerbations in adults: Systematic review and meta-analysis. *Allergy Asthma Proc.* **35**, 278–287 (2014).
19. T. Liu *et al*., Type 2 cysteinyl leukotriene receptors drive IL-33-dependent type 2 immunopathology and aspirin sensitivity. *J. Immunol.* **200**, 915–927 (2018).
20. E. Duah *et al*., Cysteinyl leukotriene 2 receptor promotes endothelial permeability, tumor angiogenesis, and metastasis. *Proc. Natl. Acad. Sci. U.S.A.* **116**, 199–204 (2019).
21. T. Andoh, Y. Kuraishi, Intradermal leukotriene B4, but not prostaglandin E2, induces itch-associated responses in mice. *Eur. J. Pharmacol.* **353**, 93–96 (1998).
22. T. Andoh *et al*., Involvement of leukotriene B4 in itching in a mouse model of ocular allergy. *Exp. Eye Res.* **98**, 97–103 (2012).
23. T. Trang, B. McNaull, R. Quirion, K. Jhamandas, Involvement of spinal lipoxygenase metabolites in hyperalgesia and opioid tolerance. *Eur. J. Pharmacol.* **491**, 21–30 (2004).
24. S. Zinn *et al*., The leukotriene B4 receptors BLT1 and BLT2 form an antagonistic sensitizing system in peripheral sensory neurons. *J. Biol. Chem.* **292**, 6123–6134 (2017).
25. F. Cevikbas, E. A. Lerner, Physiology and pathophysiology of itch. *Physiol. Rev.* **100**, 945–982 (2020).
26. W. S. Shim *et al*., TRPV1 mediates histamine-induced itching via the activation of phospholipase A2 and 12-lipoxygenase. *J. Neurosci.* **27**, 2331–2337 (2007).
27. P. J. Dunford *et al*., Histamine H4 receptor antagonists are superior to traditional antihistamines in the attenuation of experimental pruritus. *J. Allergy Clin. Immunol.* **119**, 176–183 (2007).
28. F. Cevikbas *et al*., A sensory neuron-expressed IL-31 receptor mediates T helper cell-dependent itch: Involvement of TRPV1 and TRPA1. *J. Allergy Clin. Immunol.* **133**, 448–460 (2014).
29. L. K. Oetjen *et al*., Sensory neurons Co-opt classical immune signaling pathways to mediate chronic itch. *Cell* **171**, 217–228.e13 (2017).
30. L. Han *et al*., A subpopulation of nociceptors specifically linked to itch. *Nat. Neurosci.* **16**, 174–182 (2013).
31. D. Usoskin *et al*., Unbiased classification of sensory neuron types by large-scale single-cell RNA sequencing. *Nat. Neurosci.* **18**, 145–153 (2015).
32. A. Zeisel *et al*., Molecular architecture of the mouse nervous system. *Cell* **174**, 999–1014.e22 (2018).
33. Q. Liu *et al*., Mechanisms of itch evoked by β-alanine. *J. Neurosci.* **32**, 14532–14537 (2012).
34. K. K. Stantcheva *et al*., A subpopulation of itch-sensing neurons marked by ret and somatostatin expression. *EMBO Rep.* **17**, 585–600 (2016).
35. J. Huang *et al*., Circuit dissection of the role of somatostatin in itch and pain. *Nat. Neurosci.* **21**, 707–716 (2018).
36. S. K. Mishra, M. A. Hoon, The cells and circuitry for itch responses in mice. *Science* **340**, 968–971 (2013).
37. C. L. Li *et al*., Somatosensory neuron types identified by high-coverage single-cell RNA-sequencing and functional heterogeneity. *Cell Res.* **26**, 967 (2016).
38. N. Sharma *et al*., The emergence of transcriptional identity in somatosensory neurons. *Nature* **577**, 392–398 (2020).
39. I. M. Chiu *et al*., Transcriptional profiling at whole population and single cell levels reveals somatosensory neuron molecular diversity. *eLife* **3**, e04660 (2014).
40. E. Sonkoly *et al*., IL-31: A new link between T cells and pruritus in atopic skin inflammation. *J. Allergy Clin. Immunol.* **117**, 411–417 (2006).
41. H. J. Solinski *et al*., Nppb neurons are sensors of mast cell-induced itch. *Cell Rep.* **26**, 3561–3573.e4 (2019).
42. J. Meixiong, X. Dong, Mas-related G protein-coupled receptors and the biology of itch sensation. *Annu. Rev. Genet.* **51**, 103–121 (2017).
43. S. G. Shimada, R. H. LaMotte, Behavioral differentiation between itch and pain in mouse. *Pain* **139**, 681–687 (2008).
44. J. Meixiong *et al*., Activation of mast cell-expressed Mas-related G-1 protein coupled receptors drives non histaminergic itch. *Immunity* **50**, 1163–1171.e5 (2019).
45. H. Pan *et al*., Identification of a spinal circuit for mechanical and persistent spontaneous itch. *Neuron* **103**, 1135–1149.e6 (2019).
46. K. Sakai, T. Akiyama, New insights into the mechanisms behind mechanical itch. *Exp. Dermatol.* **29**, 680–686 (2020).
47. E. A. Mellor *et al*., Expression of the type 2 receptor for cysteinyl leukotrienes (CysLT2R) by human mast cells: Functional distinction from CysLT1R. *Proc. Natl. Acad. Sci. U.S.A.* **100**, 11589–11593 (2003).
48. S. A. Oldford, J. S. Marshall, Mast cells as targets for immunotherapy of solid tumors. *Mol. Immunol.* **63**, 113–124 (2015).
49. S. R. Wilson *et al*., TRPA1 is required for histamine-independent, Mas-related G protein-coupled receptor-mediated itch. *Nat. Neurosci.* **14**, 595–602 (2011).
50. C. Perner *et al*., Substance P release by sensory neurons triggers dendritic cell migration and initiates the type-2 immune response to allergens. *Immunity* **53**, 1063–1077.e7 (2020).
51. G. Yosipovitch *et al*., Skin barrier damage and itch: Review of mechanisms, topical management and future directions. *Acta Derm. Venereol.* **99**, 1201–1209 (2019).
52. M. Li *et al*., Topical vitamin D3 and low-calcemic analogs induce thymic stromal lymphopoietin in mouse keratinocytes and trigger an atopic dermatitis. *Proc. Natl. Acad. Sci. U.S.A.* **103**, 11736–11741 (2006).
53. T. Morita *et al*., HTR7 mediates serotonergic acute and chronic itch. *Neuron* **87**, 124–138 (2015).
54. C. M. Walsh *et al*., Neutrophils promote CXCR3-dependent itch in the development of atopic dermatitis. *eLife* **8**, e48448 (2019).
55. T. Voisin, A. Bouvier, I. M. Chiu, Neuro-immune interactions in allergic diseases: Novel targets for therapeutics. *Int. Immunol.* **29**, 247–261 (2017).
56. N. A. Soter, R. A. Lewis, E. J. Corey, K. F. Austen, Local effects of synthetic leukotrienes (LTC4, LTD4, LTE4, and LTB4) in human skin. *J. Invest. Dermatol.* **80**, 115–119 (1983).
57. S. F. Talbot, P. C. Atkins, E. J. Goetzl, B. Zweiman, Accumulation of leukotriene C4 and histamine in human allergic skin reactions. *J. Clin. Invest.* **76**, 650–656 (1985).
58. Z. Hua, H. Fei, X. Mingming, Evaluation and interference of serum and skin lesion levels of leukotrienes in patients with eczema. *Prostaglandins Leukot. Essent. Fatty Acids* **75**, 51–55 (2006).
59. Y. Jiang, L. A. Borrelli, Y. Kanaoka, B. J. Bacskai, J. A. Boyce, CysLT2 receptors interact with CysLT1 receptors and down-modulate cysteinyl leukotriene dependent mitogenic responses of mast cells. *Blood* **110**, 3263–3270 (2007).
60. T. Liu *et al*., Leukotriene D(4) paradoxically limits LTC(4) driven platelet activation and lung immunopathology. *J. Allergy Clin. Immunol.* 10.1016/j.jaci.2020.10.041 (2020).
61. A. D. Green, K. K. Young, S. G. Lehto, S. B. Smith, J. S. Mogil, Influence of genotype, dose and sex on pruritogen-induced scratching behavior in the mouse. *Pain* **124**, 50–58 (2006).
62. S. Naik *et al*., Regulation of cysteinyl leukotriene type 1 receptor internalization and signaling. *J. Biol. Chem.* **280**, 8722–8732 (2005).
63. D. A. Deshpande *et al*., PKC-dependent regulation of the receptor locus dominates functional consequences of cysteinyl leukotriene type 1 receptor activation. *FASEB J.* **21**, 2335–2342 (2007).
64. J. Agier, S. Różalska, K. Wódz, E. Brzezińska-Błaszczyk, Leukotriene receptor expression in mast cells is affected by their agonists. *Cell. Immunol.* **317**, 37–47 (2017).
65. T. J. Price, C. M. Flores, Critical evaluation of the colocalization between calcitonin gene-related peptide, substance P, transient receptor potential vanilloid subfamily type 1 immunoreactivities, and isolectin B4 binding in primary afferent neurons of the rat and mouse. *J. Pain* **8**, 263–272 (2007).
66. S. Shiers, R. M. Klein, T. J. Price, Quantitative differences in neuronal subpopulations between mouse and human dorsal root ganglia demonstrated with RNAscope in situ hybridization. *Pain* **161**, 2410–2424 (2020).
67. M. Okubo *et al*., Expression of leukotriene receptors in the rat dorsal root ganglion and the effects on pain behaviors. *Mol. Pain* **6**, 57 (2010).
68. T. E. Taylor-Clark, C. Nassenstein, B. J. Undem, Leukotriene D4 increases the excitability of capsaicin-sensitive nasal sensory nerves to electrical and chemical stimuli. *Br. J. Pharmacol.* **154**, 1359–1368 (2008).
69. D. Keppler, M. Huber, T. Baumert, A. Guhlmann, Metabolic inactivation of leukotrienes. *Adv. Enzyme Regul.* **28**, 307–319 (1989).
70. J. Z. Haeggström, Leukotriene biosynthetic enzymes as therapeutic targets. *J. Clin. Invest.* **128**, 2680–2690 (2018).
71. R. J. Soberman, P. Christmas, The organization and consequences of eicosanoid signaling. *J. Clin. Invest.* **111**, 1107–1113 (2003).
72. T. C. Moon, A. D. Befus, M. Kulka, Mast cell mediators: Their differential release and the secretory pathways involved. *Front. Immunol.* **5**, 569 (2014).
73. N. Serhan *et al*., House dust mites activate nociceptor-mast cell clusters to drive type 2 skin inflammation. *Nat. Immunol.* **20**, 1435–1443 (2019).
74. T. Miyamoto, H. Nojima, T. Shinkado, T. Nakahashi, Y. Kuraishi, Itch-associated response induced by experimental dry skin in mice. *Jpn. J. Pharmacol.* **88**, 285–292 (2002).
75. D. P. Woodmansee, R. A. Simon, A pilot study examining the role of zileuton in atopic dermatitis. *Ann. Allergy Asthma Immunol.* **83**, 548–552 (1999).
76. A. Y. Pei, H. H. Chan, T. F. Leung, Montelukast in the treatment of children with moderate-to-severe atopic dermatitis: a pilot study. *Pediatr. Allergy Immunol.* **12**, 154–158 (2001).
77. P. S. Friedmann *et al*., A double-blind, placebo-controlled trial of montelukast in adult atopic eczema. *Clin. Exp. Allergy* **37**, 1536–1540 (2007).
78. E. Nettis, A. Pannofino, M. Fanelli, A. Ferrannini, A. Tursi, Efficacy and tolerability of montelukast as a therapeutic agent for severe atopic dermatitis in adults. *Acta Derm. Venereol.* **82**, 297–298 (2002).
79. Y. H. Jeon, T. K. Min, H. J. Yang, B. Y. Pyun, A double-blind, randomized, crossover study to compare the effectiveness of montelukast on atopic dermatitis in Korean children. *Allergy Asthma Immunol. Res.* **8**, 305–311 (2016).
80. S. R. Wilson *et al*., The ion channel TRPA1 is required for chronic itch. *J. Neurosci.* **33**, 9283–9294 (2013).
81. M. A. Gijón, S. Zarini, R. C. Murphy, Biosynthesis of eicosanoids and transcellular metabolism of leukotrienes in murine bone marrow cells. *J. Lipid Res.* **48**, 716–725 (2007).
82. S. Zarini, M. A. Gijón, A. E. Ransome, R. C. Murphy, A. Sala, Transcellular biosynthesis of cysteinyl leukotrienes in vivo during mouse peritoneal inflammation. *Proc. Natl. Acad. Sci. U.S.A.* **106**, 8296–8301 (2009).